

# Magneto-elastic oscillations and the damping of crustal shear modes in magnetars

Michael Gabler<sup>1,2,3</sup>, Pablo Cerdá-Durán<sup>1</sup>, José A. Font<sup>2</sup>, Ewald Müller<sup>1</sup>  
and Nikolaos Stergioulas<sup>3</sup>

<sup>1</sup>*Max-Planck-Institut für Astrophysik, Karl-Schwarzschild-Str. 1, 85741 Garching, Germany*

<sup>2</sup>*Departamento de Astronomía y Astrofísica, Universidad de Valencia, 46100 Burjassot (Valencia), Spain*

<sup>3</sup>*Department of Physics, Aristotle University of Thessaloniki, Thessaloniki 54124, Greece*

26 October 2018

## ABSTRACT

In a realistic model of magneto-elastic oscillations in magnetars, we find that crustal shear oscillations, often invoked as an explanation of quasi-periodic oscillations (QPOs) seen after giant flares in soft gamma-ray repeaters (SGRs), are damped by resonant absorption on timescales of at most 0.2s, for a lower limit on the dipole magnetic field strength of  $5 \times 10^{13}$ G. At higher magnetic field strengths (typical in magnetars) the damping timescale is even shorter, as anticipated by earlier toy-models. We have investigated a range of equations of state and masses and if magnetars are dominated by a dipole magnetic field, our findings exclude torsional shear oscillations of the crust from explaining the observed low-frequency QPOs. In contrast, we find that the Alfvén QPO model is a viable explanation of observed QPOs, if the dipole magnetic field strength exceeds a minimum strength of about several times  $10^{14}$ G to  $10^{15}$ G. Then, Alfvén QPOs are no longer confined to the fluid core, but completely dominate in the crust region and have a maximum amplitude at the surface of the star.

**Key words:** MHD - stars: magnetic field - stars: neutron - stars: oscillations - stars: flare - stars: magnetars

## 1 INTRODUCTION

The observation of giant flares in soft gamma-ray repeaters (SGRs; compact objects with very strong magnetic fields or magnetars (Duncan & Thompson 1992)) may open a gateway towards the exciting field of neutron star seismology. In the decaying X-ray tail of two such events, SGR 1900+14 and SGR 1806-20, a number of long-lasting, quasi-periodic oscillations (QPOs) have been observed (see Israel et al. (2005) and Watts & Strohmayer (2007) for recent reviews). Early models interpreted the observed QPO frequencies as directly related to torsional shear oscillations of the solid crust of a neutron star excited during a giant flare event (see Duncan (1998); Strohmayer & Watts (2005); Piro (2005); Sotani et al. (2007); Samuelsson & Andersson (2007), and references therein) raising hopes that through their identification, the physical properties of the crust could be probed (Steiner & Watts 2009). Due to the extremely strong magnetic fields present in magnetars, however, a self-consistent model that includes global magnetohydrodynamic (MHD) oscillations interacting with the shear oscillations of the crust is required (Levin (2006), Glampedakis & Andersson (2006), Levin (2007), Lee (2007, 2008)). In a highly simplified model, Levin (2007) showed that shear oscillations will be absorbed by an MHD continuum of Alfvén oscillations, while long-lived QPOs may still appear at the turning points or edges of the continuum.

Sotani et al. (2008b) and subsequently Cerdá-Durán et al. (2009) (see also Colaiuda et al. (2009)), using a more realistic, general-relativistic MHD model but still ignoring an extended crust, found two families of Alfvén QPOs related to turning points of the frequency of torsional Alfvén waves near the magnetic pole and inside a region of closed magnetic field lines near the equator. Each QPO family consists of two sub-families differing by their symmetry behaviour with respect to the equatorial plane. The results of the numerical simulations were explained by a semi-analytic model based on standing waves in the short-wavelength limit (Cerdá-Durán et al. 2009). The Alfvén QPO model is very attractive, because it reproduces the near-integer-ratios of the observed 30, 92 and 150 Hz frequencies in SGR 1806-20, at magnetic field strengths expected for magnetars. In this model, the observed SGR QPOs, rather than probing the crust, yield information on the magnetic field and the compactness of the star.

The omission of an extended crust in the previous studies of Sotani et al. (2008b), Cerdá-Durán et al. (2009), and Colaiuda et al. (2009) can be considered as a limiting case of a very strong magnetic field. For intermediate magnetic field strengths, however, an understanding of magnetar oscillations requires the inclusion of crust-core coupling. In this Letter, we present the first such realistic simulations of coupled, magneto-elastic oscillations. We use a general-relativistic framework, a dipolar magnetic field, and a tabu-

lated equation of state (EOS) for dense matter. The numerical simulations are based on state-of-the-art Riemann solver methods for both the interior MHD fluid and the crust. A recent study by van Hoven & Levin (2010) also takes entanglement of magnetic field lines into account, thereby generalising the toy model of Levin (2007). Some first results on coupled crust-core oscillations also appeared in Kokkotas et al. (2010).

We use units where  $c = G = 1$  with  $c$  and  $G$  being the speed of light and the gravitational constant, respectively. Latin (Greek) indices run from 1 to 3 (0 to 3).

## 2 THEORETICAL FRAMEWORK

The present study of torsional oscillations of magnetars is based on a numerical integration of the general relativistic MHD equations. As in Cerdá-Durán et al. (2009), who considered purely Alfvén oscillations of the fluid core, assume (i) a zero temperature EOS, (ii) axisymmetry, (iii) a purely poloidal magnetic field configuration, (iv) the Cowling approximation, (v) a spherically symmetric background, and (vi) small amplitude oscillations. Because of assumptions (ii) and (iii) polar oscillations decouple from axial ones in the linear regime. Therefore, we concentrate on purely axial oscillations and evolve the  $\varphi$ -component of the evolution variables only. We assume a conformally flat metric <sup>1</sup>

$$ds^2 = -\alpha^2 dt^2 + \phi^4 (dr^2 + r^2 d\theta^2 + r^2 \sin^2 \theta d\varphi^2), \quad (1)$$

where  $\alpha$  is the lapse function and  $\phi$  the conformal factor, and consider a stress-energy tensor  $T^{\mu\nu}$  of the form

$$\begin{aligned} T^{\mu\nu} &= T_{\text{fluid}}^{\mu\nu} + T_{\text{mag}}^{\mu\nu} + T_{\text{elas}}^{\mu\nu} \\ &= \rho h u^\mu u^\nu + P g^{\mu\nu} + b^2 u^\mu u^\nu + \frac{1}{2} b^2 g^{\mu\nu} - b^\mu b^\nu \\ &\quad - 2\mu_S \Sigma^{\mu\nu}, \end{aligned} \quad (2)$$

where  $\rho$  is the rest-mass density,  $h$  the specific enthalpy,  $P$  the isotropic fluid pressure,  $u^\mu$  the 4-velocity of the fluid,  $b^\mu$  the magnetic field measured by a co-moving observer (with  $b^2 := b^\mu b_\mu$ ),  $\Sigma^{\mu\nu}$  the shear tensor, and  $\mu_S$  the shear modulus. The latter is obtained according to Sotani et al. (2007).

The conservation of energy and momentum  $\nabla_\nu T^{\mu\nu} = 0$ , and the induction equation lead to the following system of evolution equations

$$\frac{1}{\sqrt{-g}} \left( \frac{\partial \sqrt{\gamma} \mathbf{U}}{\partial t} + \frac{\partial \sqrt{-g} \mathbf{F}^i}{\partial x^i} \right) = 0, \quad (3)$$

where  $g$  and  $\gamma$  are the determinants of the 4-metric and 3-metric, respectively. The two-component state and flux vectors are given by

$$\mathbf{U} = [S_\varphi, B^\varphi], \quad (4)$$

$$\mathbf{F}^r = \left[ -\frac{b_\varphi B^r}{W} - 2\mu_S \Sigma^r_\varphi, -v^\varphi B^r \right], \quad (5)$$

$$\mathbf{F}^\theta = \left[ -\frac{b_\varphi B^\theta}{W} - 2\mu_S \Sigma^\theta_\varphi, -v^\varphi B^\theta \right], \quad (6)$$

where  $B^i$  are the magnetic field components as measured by an *Eulerian observer* (Antón et al. 2006), and  $W = \alpha u^t$  is the Lorentz factor. The shear tensor  $\Sigma^{i\varphi} = 1/2 g^{ij} \xi_{,i}^\varphi$  contains the spatial derivatives (denoted by a comma) of the fluid displacement  $\xi^\varphi$  due

to the oscillations, which are related to the fluid 4-velocity according to  $\xi_{,t}^\varphi = \alpha v^\varphi = u^\varphi / u^t$ , where  $v^\varphi$  is the  $\varphi$ -component of the fluid 3-velocity. Hence, the evolution of the spatial derivatives  $\xi_{,r}^\varphi$  and  $\xi_{,\theta}^\varphi$  is given by

$$(\xi_{,k}^\varphi)_{,t} - (\alpha v^\varphi)_{,k} = 0 \quad \text{with } k \in \{r, \theta\}. \quad (7)$$

We also need to provide boundary conditions. At the surface the radial derivative of the displacement has to vanish ( $\xi_{,r}^\varphi = 0$ ), as we assume a continuous traction and vanishing surface currents. At the crust-core interface we demand the continuity of the parallel electric field, which implies a continuous displacement  $\xi^\varphi$ . Together with the continuity of the traction the latter leads to a relation between the radial derivatives of the displacement in the core and in the crust:  $\xi_{\text{core},r}^\varphi = (1 + \delta) \xi_{\text{crust},r}^\varphi$  with  $\delta = \mu_S / (b_r b^r)$ .

To construct equilibrium models we choose between different barotropic EOSs for the core that are matched to an EOS for the crust. The available models for the core are the soft EOS A (Pandharipande 1971), the intermediate EOS WFF3 (Wiringa et al. 1988), EOS APR (Akmal et al. 1998) and the stiff EOS L (Pandharipande & Smith 1975). For the low density region of the crust we choose between EOS NV (Negele & Vautherin 1973) and EOS DH (Douchin & Haensel 2001). Details about the different combinations of EOSs can be found in Sotani et al. (2007). We use a reference model with a mass of  $1.4 M_\odot$  and a circumferential radius  $R_{\text{star}} = 12.26$  km, described by the APR + DH EOS. In contrast to Sotani et al. (2007) we compute magnetised equilibrium models using the LORENE library ([www.lorene.obspm.fr](http://www.lorene.obspm.fr)).

Our simulation code is an extended version of the GRMHD code presented in Cerdá-Durán et al. (2009). It includes the shear terms as they appear in (2), and the evolution of the displacements (7). The proper working of the MHD part of the code was demonstrated in Cerdá-Durán et al. (2008). To test the extended code we compared its results obtained for two limiting cases, zero magnetic field and zero shear modulus, with those of previous studies. The purely crustal shear oscillations presented in Sotani et al. (2007) are recovered with an agreement of 1%, and the Alfvén continuum is obtained naturally as in Cerdá-Durán et al. (2009). Further details on the derivation of the model equations, the numerical methods, and the code tests will be discussed in Gabler, Cerdá-Durán, Font & Stergioulas (in preparation).

## 3 DAMPING OF CRUSTAL SHEAR MODES

To study the behaviour of coupled crust-core oscillations we perturb the equilibrium stellar model by imposing a velocity perturbation and then follow the time evolution of the system (3) - (7). Unless stated otherwise, we use a grid of  $150 \times 100$  zones in our simulations covering a domain  $[0, R_{\text{star}}] \times [0, \pi]$ . The angular grid is equidistant, while the radial grid is equidistant only in the crust, where 40 per cent of the zones are located, and coarsens towards the centre of the star. Symmetries are exploited whenever a perturbation is of purely odd or even parity with respect to the equatorial plane. We use the term *damping* in the following to refer to *resonant absorption* of crustal shear oscillations by the *Alfvén continuum* of the core (unless we explicitly refer to numerical damping caused by finite-differencing).

We investigated perturbations of different radial extent encompassing only the crust, only the core, or the whole star. Since all three types of perturbations give qualitatively similar results, we focus on whole star perturbations in the following, as this is the most generic case. We first consider initial perturbations consisting of a single torsional, spherical vector harmonics  $l$ -mode. To

<sup>1</sup> This provides a very good approximation as our neutron star models are almost perfectly spherically symmetric except for very small deviations due to the presence of an axisymmetric magnetic field.

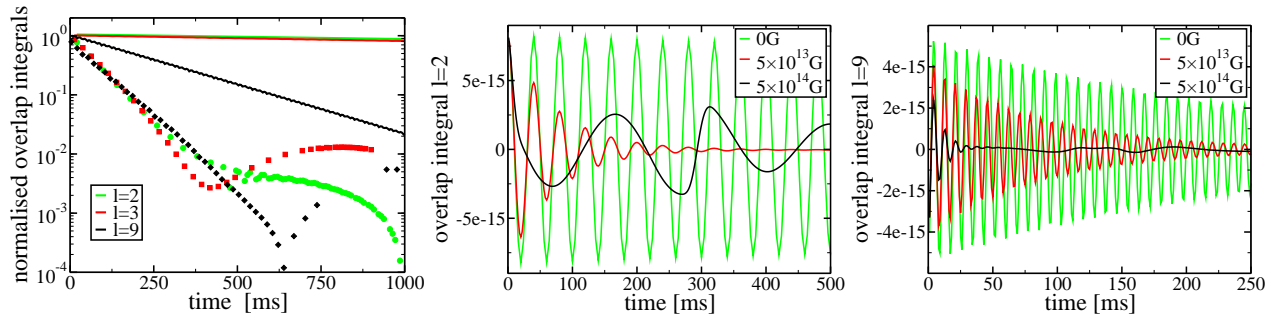


**Figure 1.** Time evolution of overlap integrals with the eigenmodes of the crust. *Left panel:* Damping of  $l = 2, 3,$  and  $9$  initial perturbations due to resonant absorption of the fundamental ( $n = 0$ ) crustal shear mode for a magnetised model with  $5 \times 10^{13}$  G (dots). In the corresponding unmagnetised models (solid lines) only numerical damping occurs which increases with the angular order  $l$  of the mode. *Middle panel:* Overlap integrals for the  $l = 2$  mode, where resonant absorption of the crustal modes becomes stronger with increasing magnetic field strength. *Right panel:* same as middle panel, but for  $l = 9$ .

$l$	2	3	9	10
$\tau$ [s] for $B = 0$	5.500	4.620	0.260	0.170
$\tau$ [s] for $B = 5 \times 10^{13}$ G	0.072	0.080	0.087	0.081
$\tau$ [s] for $B = 10^{14}$ G	0.040	0.040	0.022	0.021

**Table 1.** Damping timescales  $\tau$  due to resonant absorption of crustal shear modes by the Alfvén continuum for various initial perturbation modes  $l$ .

investigate the damping of a single crustal mode we compute *overlap integrals* of the evolved variables with mode eigenfunctions (the latter are found by solving the linear eigenvalue problem for the crustal modes, see Schumaker & Thorne (1983); Messios et al. (2001); Sotani et al. (2007)). Because the eigenmodes of the crust form a complete orthonormal set we can expand any perturbation in terms of the corresponding eigenfunctions. The expansion factors, which provide a measure of how strong each crustal mode contributes to the perturbation, are obtained via the overlap integrals with the eigenfunctions. For more details on this method see Gabler et al. (2009). In the left panel of Fig. 1 we show the maximum (absolute) amplitudes of the overlap integrals for different initial perturbations and for simulations both without magnetic field (solid lines) and with a polar magnetic field of  $5 \times 10^{13}$  G (dots). In the field-free case the lines represent the *numerical damping* of crustal modes due to finite-differencing. When a magnetic field is present, the damping (now due to resonant absorption) increases with the magnetic field strength.

For all modes, the timescale of resonant absorption is much shorter than that of numerical damping (see Table 1). After about 500 ms, the overlap integrals no longer sample the crust oscillations, but instead the magneto-elastic oscillations which then dominate the evolution (see below).

The middle and right panels of Fig. 1 show the overlap integrals for  $l = 2$  and  $l = 9$  modes of the crust as a function of time for different magnetic field strengths, respectively. For  $l = 2$  and  $B = 5 \times 10^{13}$  G we find almost complete damping of the crustal mode after  $\sim 0.5$  s. For a stronger magnetic field ( $B = 5 \times 10^{14}$  G) the crustal mode becomes already damped after less than one oscillation, and only the dominant magneto-elastic oscillations remain. Similar statements hold for the evolution of the  $l = 9$  perturbation. However, in that case it takes a few oscillations before the crustal mode is damped, even for  $B = 5 \times 10^{14}$  G.

We also analysed a more general initial perturbation consisting of a mixture of  $l = 2$  up to  $l = 10$  modes, which excites a large number of crustal modes of different angular order  $l$  and ra-

EOS	$\tau$ [ms] at $B = 10^{14}$ G		
	$n = 0, l = 2$	$n = 0, l = 3$	$n = 0, l = 9$
A+DH 1.6	23	23	15
A+NV 1.6	39	43	75
APR+DH 2.0	32	31	17
APR+NV 2.0	50	54	80
L+DH 1.6	50	52	24
L+NV 1.6	79	86	53
L+DH 2.0	44	46	21
L+NV 2.0	73	80	87
W+DH 1.6	29	30	14
W+NV 1.6	53	58	69

**Table 2.** Damping timescales  $\tau$  due to resonant absorption of crustal shear modes by the Alfvén continuum for initial perturbation modes  $l = 2, l = 3$  and  $l = 9$  and for different combinations of equations of state at  $B = 10^{14}$  G. The number in the labelling of the EOS represents the mass of the neutron star model in  $M_{\odot}$ .

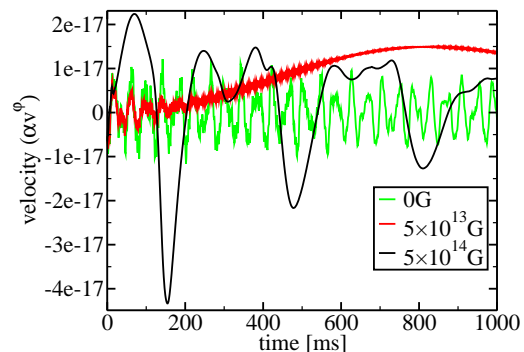


**Figure 2.** Evolution of  $\alpha v^{\varphi}$  in the crust at  $\theta = \pi/4$  for initial data containing a large number of different perturbation modes. For vanishing magnetic field, only crustal modes are excited. For  $B = 5 \times 10^{13}$  G the crustal oscillations are strongly damped, and for a ten times stronger magnetic field ( $B = 5 \times 10^{14}$  G) magneto-elastic oscillations dominate the evolution from the start.

dial order  $n$ . Fig. 2 shows the resulting evolution of the velocity in the crust at  $\theta = \pi/4$ . For the unmagnetised model, low frequency, fundamental ( $n = 0$ ) oscillations can easily be distinguished from higher frequency overtones with  $n \geq 1$ . When increasing the magnetic field strength to  $5 \times 10^{13}$  G the lower frequency modes are completely damped after  $\sim 250$  ms, whereas the higher frequency

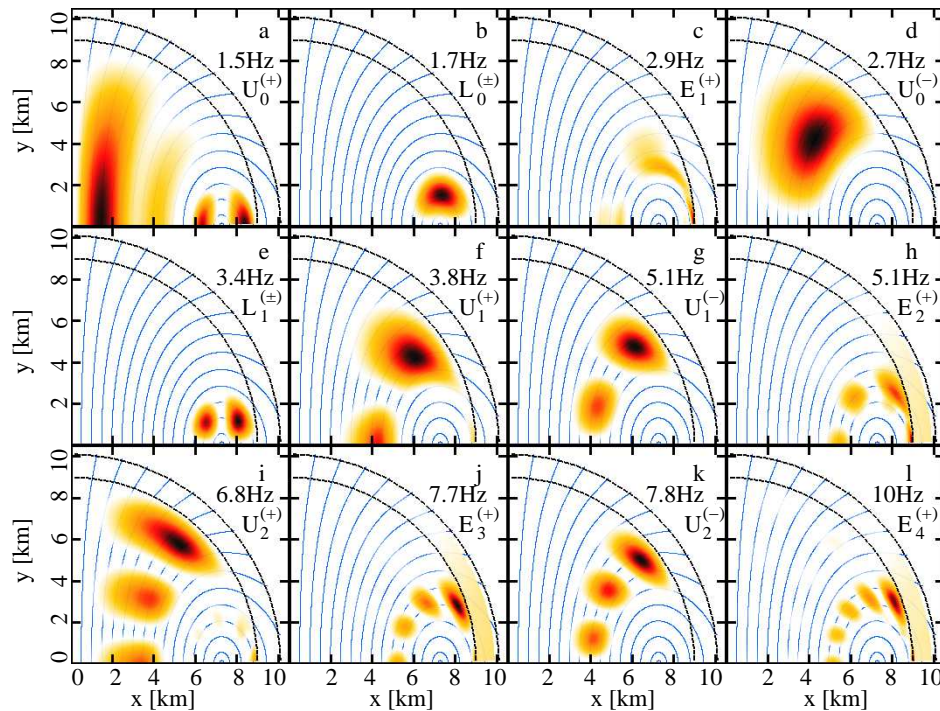


**Figure 3.** Spatial distribution of Fourier amplitudes at several QPO frequencies. Three different types of QPOs are present: (i) upper QPOs in panels *a, d, f, g, i, and k*; (ii) lower QPOs in panels *b and e*; (iii) edge QPOs in panels *c, h, j, and l*. The two black dashed lines mark the location of the crust, while the blue lines represent magnetic field lines. The colour scale ranges from zero amplitude (white) to maximum amplitude (black).

overtone survives for a longer time. In the long run, a low frequency ( $\sim 0.3$  Hz) magneto-elastic oscillation dominates. At the largest magnetic field strength shown here,  $5 \times 10^{14}$  G, there is no sign of either low or high frequency crustal modes, the evolution being completely dominated by magneto-elastic oscillations.

Damping timescales of  $n = 0$ ,  $l = \{2, 3, 9\}$  modes for different EOSs are listed in Table 2. For all EOSs and masses studied here, we find significant damping of the crustal shear modes at  $B = 10^{14}$  G. Up to the highest-order  $l = 9$  mode, the damping timescales are shorter than 0.1s. From the results in Tables 1 and 2, we deduce that even at  $B = 5 \times 10^{13}$  G, which is up to two orders of magnitude weaker than assumed magnetar field strengths, the damping timescale is *shorter than 0.2s*, which is more than two orders of magnitude shorter than the duration of observed QPOs.

#### 4 LONG-TERM QPOS

Besides the damping of crustal modes, we observe long-lasting oscillations in the fluid core of the magnetar. These *long-term QPOs* are identified by local maxima in Fourier space. Let us consider an intermediate magnetic field strength of  $4 \times 10^{14}$  G, where both the magnetic field and the crust influence the dynamics. As in the case without crust (Sotani et al. 2008b; Cerdá-Durán et al. 2009) we find two different families of long-term QPOs, as demonstrated in Fig. 3, which shows the spatial distribution of Fourier amplitudes at several QPO frequencies. The *lower* QPOs ( $L_n^{(\pm)}$ ) are located inside the region of closed field lines, while the *upper* QPOs ( $U_n^{(\pm)}$ ) concentrate along open magnetic field lines closer to the poles. We computed QPOs of either odd ( $-$ ) or even ( $+$ ) parity w.r.t. the equatorial plane, which allows for a better identification of QPOs of similar frequency but opposite parity.

The lower QPOs (Fig. 3, panels *b* and *e*) appear to be similar to those found for models without crust, except that they are limited to

the region of closed magnetic field lines inside the core. The upper QPOs are influenced by the presence of the crust in several ways. First, they are limited to the fluid region, and become vanishingly small at the base of the crust (Fig. 3, panels *a, d, f, g, i, and k*), where they are reflected. This behaviour is similar to that caused by the boundary conditions in Sotani et al. (2008b), and differs from that of the pure fluid case considered in Cerdá-Durán et al. (2009). In the latter work the continuous traction boundary condition imposed at the surface of the star resulted in a strong displacement there. Their different behaviour at the base of the crust (w.r.t. the pure fluid case in Cerdá-Durán et al. (2009)) causes a rearrangement of the QPOs. Here, the lowest frequency QPO (panel *a*) is symmetric w.r.t. the equatorial plane (even parity) - while it did not exist at all in Cerdá-Durán et al. (2009) - and the lowest-frequency QPO has odd parity.

While QPOs are located close to the symmetry axis of the field (polar axis) in models without crust (Sotani et al. 2008b; Cerdá-Durán et al. 2009), they are attached to field lines crossing the equator at around 4 km in our models including the crust. Apparently the strong coupling introduced by the crust complicates the oscillatory behaviour of the field lines, such that the interaction between neighbouring polar field lines prevents the QPOs from being established.

Furthermore, we find a new family of QPOs (Fig. 3, panels *c, h, j, and l*) connected to the last open field line of the fluid core, each member representing the lower-frequency edge of an Alfvén continuum along the open field lines. QPOs at similar locations were also identified in simulations by Colaiuda et al. (2009) without a crust.

## 5 DISCUSSION

In this Letter we have presented the first numerical simulations of axisymmetric, torsional, magneto-elastic oscillations in a realistic magnetar model, including an extended crust.

We focus on the timescales for resonant absorption of low frequency,  $n = 0$  crustal shear modes by the Alfvén continuum of the core and find that even at  $B = 5 \times 10^{13}$  G, which is up to two orders of magnitude weaker than assumed magnetar field strengths, the damping timescale is shorter than 0.2s, which is more than two orders of magnitude shorter than the duration of observed QPOs. Furthermore, the crust EOSs NV and DH which we have used have a very high shear modulus, compared to a range of other proposed EOSs (Steiner & Watts 2009). Comparing the damping timescales obtained here for the NV and DH EOSs, we find that, at a given magnetic field strength, a lower shear modulus results in a shorter damping timescale due to resonant absorption. Thus, for lower values of the shear modulus than considered here, the deduced damping timescales would be even shorter than our current findings. In addition, no significant excitation of crustal modes by the Alfvén continuum was observed at the end of our simulations, which reached up to several seconds. The above results do not leave much room for shear modes of the crust to be able to sustain oscillations that lead to significant modulations in the X-ray tail of giant SGR bursts lasting for several tens of seconds, when the magnetic field is global. The case of magnetic field configurations confined to the crust, which may be realised if the core is a type I superconductor, requires further investigation.

In contrast to the shear modes, the Alfvén QPO model (see Levin (2007); Sotani et al. (2008b); Cerdá-Durán et al. (2009); Colaiuda et al. (2009)) has several attractive features, matching to observed frequencies for a dipole field strength up to several times  $10^{15}$  G and explaining the observed integer ratios for the frequencies of QPOs. Here we find that for magnetic field strengths less than about  $10^{15}$  G, the Alfvén QPOs are mostly confined to the fluid core. For EOSs with a smaller shear modulus, this could reduce to several times  $10^{14}$  G. Above this *minimum field strength*, Alfvén oscillations completely dominate in the crust and the resulting QPOs have a maximum amplitude at the surface of the star. It is thus likely, that the Alfvén QPO model can operate efficiently only above such a minimum field strength. In that case, the possible strength of magnetar magnetic fields is limited to a narrow range, between the minimum strength discussed here and the upper bound determined in Cerdá-Durán et al. (2009). Furthermore, the empirical formulas for the QPO frequencies presented in Cerdá-Durán et al. (2009) could be used to directly constrain the strength of the magnetic field and the compactness of the star.

A more extended investigation of the minimum magnetic field strength for the Alfvén QPO model will appear in Gabler et al. (2010). We are also planning to extend our model by taking into account additional effects, such as different magnetic field topologies (see also Sotani et al. (2008a)), the coupling of the interior dynamics to an external magnetosphere, and the effect of field-line entanglement in the core.

## ACKNOWLEDGEMENTS

We are grateful to the anonymous referee for useful comments which helped to improve the final version of this letter. This work was supported by the Collaborative Research Center on Gravitational Wave Astronomy of the Deutsche Forschungsgemeinschaft

(DFG SFB/Transregio 7), the Spanish *Ministerio de Educación y Ciencia* (AYA 2007-67626-C03-01), the ESF grant COMPSTAR and a DAAD exchange grant. Computing time was provided by the *Servicio de Informática de la Universidad de Valencia*.

## REFERENCES

- Akmal A., Pandharipande V. R., Ravenhall D. G., 1998, *Phys. Rev. C*, 58, 1804
- Antón L., Zanotti O., Miralles J. A., Martí J. M., Ibáñez J. M., Font J. A., Pons J. A., 2006, *ApJ*, 637, 296
- Cerdá-Durán P., Font J. A., Antón L., Müller E., 2008, *A&A*, 492, 937
- Cerdá-Durán P., Stergioulas N., Font J. A., 2009, *MNRAS*, 397, 1607
- Colaiuda A., Beyer H., Kokkotas K. D., 2009, *MNRAS*, 396, 1441
- Douchin F., Haensel P., 2001, *A&A*, 380, 151
- Duncan R. C., 1998, *ApJ*, 498, L45+
- Duncan R. C., Thompson C., 1992, *ApJ*, 392, L9
- Gabler M., Cerdá-Durán P., Font J., Stergioulas N., 2010, in preparation
- Gabler M., Spherhake U., Andersson N., 2009, *Phys. Rev. D*, 80, 064012
- Glampedakis K., Andersson N., 2006, *MNRAS*, 371, 1311
- Israel G. L., Belloni T., Stella L., Rephaeli Y., Gruber D. E., Casella P., Dall’Osso S., Rea N., Persic M., Rothschild R. E., 2005, *ApJ*, 628, L53
- Kokkotas K. D., Gaertig E., Colaiuda A., 2010, *Journal of Physics: Conference Series*, 222, 012031
- Lee U., 2007, *MNRAS*, 374, 1015
- Lee U., 2008, *MNRAS*, 385, 2069
- Levin Y., 2006, *MNRAS*, 368, L35
- Levin Y., 2007, *MNRAS*, 377, 159
- Messios N., Papadopoulos D. B., Stergioulas N., 2001, *MNRAS*, 328, 1161
- Negele J. W., Vautherin D., 1973, *Nuclear Physics A*, 207, 298
- Pandharipande V. R., 1971, *Nuclear Physics A*, 178, 123
- Pandharipande V. R., Smith R. A., 1975, *Physics Letters B*, 59, 15
- Piro A. L., 2005, *ApJ*, 634, L153
- Samuelsson L., Andersson N., 2007, *MNRAS*, 374, 256
- Schumaker B. L., Thorne K. S., 1983, *MNRAS*, 203, 457
- Sotani H., Colaiuda A., Kokkotas K. D., 2008a, *MNRAS*, 385, 2161
- Sotani H., Kokkotas K. D., Stergioulas N., 2007, *MNRAS*, 375, 261
- Sotani H., Kokkotas K. D., Stergioulas N., 2008b, *MNRAS*, 385, L5
- Steiner A. W., Watts A. L., 2009, *Physical Review Letters*, 103, 181101
- Strohmayer T. E., Watts A. L., 2005, *ApJ*, 632, L111
- van Hoven M., Levin Y., 2010, *Magnetar Oscillations I: strongly coupled dynamics of the crust and the core*, arXiv:1006.0348
- Watts A. L., Strohmayer T. E., 2007, *Advances in Space Research*, 40, 1446
- Wiringa R. B., Fiks V., Fabrocini A., 1988, *Phys. Rev. C*, 38, 1010